Surface core-level shifts on Ge(100): $c(4\times2)$ to 2×1 and 1×1 phase transitions

G. Le Lay*
Centre de Recherche sur les Mécamismes de la Croissance Cristalline, Campus de Luminy Case 913, 13288 Marseille CEDEX 09, France

J. Kanski and P. O. Nilsson
Department of Physics, Chalmers University of Technology, S-41296 Goteborg, Sweden

U. O. Karlsson
MAX-Lab, University of Lund, Box 118, S-22100 Lund, Sweden

K. Hricovini
Laboratoire pour l'Utilisation du Rayonnement Électromagnétique, Bâtiment 209D, 91405 Orsay CEDEX, France
(Received 4 June 1991)

By comparing, under identical experimental conditions, high-resolution synchrotron-radiation core-level photoemission spectra taken from both Ge(111) and Ge(100) samples, we establish that the decomposition of the Ge $3d$ lines from the clean Ge(100) 2×1 surface at room temperature requires two surface components shifted by -0.23 and -0.60 eV relative to the bulk one. This deconvolution is fully consistent with the asymmetric-dimer reconstruction model of this surface. We further study the reversible phase transitions that occur on this surface: $2\times1\leftrightarrow c(4\times2)$ at low temperature; $2\times1\leftrightarrow1\times1$ at high temperature. We show from both core-level and valence-band studies that the number of dimer bonds is essentially conserved in these transitions. We also suggest, by comparing a dimer with an Ising spin, that these transitions correspond, respectively, to an antiferromagnetic ordering at low temperatures and to a paramagnetic disordering at high temperatures.

I. INTRODUCTION

The atoms at an unreconstructed Ge(100) surface, as at a Si(100) surface, have two broken bonds. It is energetically favorable for neighboring atoms to move together to form new bonds. This process leads to buckled asymmetric dimers seen in scanning tunneling microscopy (STM) (Ref. 1) and to the formation of 2×1 and higher-order $p(2\times2)$, $c(2\times2)$, and $c(4\times2)$ reconstructions. Kevan[2] has reported in a low-energy electron-diffraction (LEED) and photoemission study a phase transition from $c(4\times2)$ to 2×1 symmetry at 220 K, while Johnson *et al.*[3] showed recently with surface x-ray diffraction that the Ge(100) surface undergoes a further reversible $2\times1\leftrightarrow1\times1$ transition at 955 K.

In a detailed angle-resolved (AR) photoemission study of the surface electronic structure of Ge(100) 2×1 dangling-bond bands, surface bands derived from the dimer bond and from different backbonds have been identified upon comparison with self-consistent calculations of the surface band structure based on the asymmetric-dimer model.[4] In core-level photoemission the dimer-atom contribution can be seen as a shoulder on the high-kinetic-energy side of the spectra.[5,6] This technique has been employed in recent years to study the phase transitions on the clean Ge(111) surface[7,8] at high temperatures.

To our knowledge, core-level photoemission of the Ge(100) surface has been limited to the 2×1 structure at room-temperature (RT). Since the usefulness of a local probe like core-level spectroscopy has been established in the study of the phase transitions of Ge(111), we use a combined valence-band and core-level photoemission study of the surface phase transitions on Ge(100). We look in detail at a crucial point: the surface core-level shifts for the different structures. Up until now a single surface-shifted component has been considered in the Ge $3d$ core-level decomposition of the RT 2×1 surface.[5,6,9,10] This conflicts with existing theory,[11] which predicts a charge transfer from the down atom to the up atom in the dimer. On this basis, at least two surface shifts would be expected. In fact, using very high resolution, Wertheim *et al.*[12] showed that for the corresponding Si(100) 2×1 surface the Si $2p$ photoemission spectra exhibit two surface features, one above and one below the bulk line.

We will prove that two surface features are also present on the Ge(100) 2×1 surface and that they are conserved during the two reversible phase transitions: $c(4\times2)\leftrightarrow2\times1$ at LT, $2\times1\leftrightarrow1\times1$ at high temperature (HT).

II. EXPERIMENT

The experiments have been performed at two synchrotron radiation facilities. At MAX-Lab, Lund, Sweden, at beam line 41 we have reexamined the Ge(100) 2×1 reconstruction at RT and studied the high-temperature $2\times1\leftrightarrow1\times1$ phase transition. At the Laboratoire pour l'Utilisation du Rayonnement Électromagnétique, Orsay,

 ©1992 The American Physical Society

France at the undulator SU6 beam line of the Super-ACO storage ring where the photoemission chamber permits low-temperature measurements, we studied the $c(4\times2)\leftrightarrow2\times1$ phase transition. Both chambers on these two photoemission lines are equipped with an angle-resolving ($<2°$ acceptance angle) spectrometer and the settings were such as to ensure approximately the same total experimental energy resolution (monochromator and analyzer) 0.25–0.30 eV in the whole range of photon energies used (17–90 eV), as measured many times from the Fermi-edge width of a clean tantalum foil in contact with the germanium samples. In Lund we mounted for comparison on the same holder (standard molecular-beam-epitaxy-type molybloc system) two lightly doped n-type germanium crystals: one Ge(100) and one Ge(111). A thermocouple spot-welded on the molybloc gave a temperature reference. We made sure that we passed the temperature of the $2\times1\leftrightarrow1\times1$ phase transition by carefully examining the LEED patterns upon cooling, at which point light does not obscure the appearance of half-order spots. At LURE we used p-type Ge(100) samples mounted on a rod that permitted cooling to liquid-nitrogen temperature (LNT). By argon-ion bombardment at 500 °C and subsequent annealing at 700 °C we obtained excellent $c(2\times8)$ LEED patterns on the (111) crystals and very sharp two-domain 2×1 patterns on the Ge(100) crystals at RT. At LNT we observed sharp quarter-order spots and very good $c(4\times2)$ patterns on the Ge(100) crystals.

III. RESULTS OBTAINED AT RT

In Fig. 1 we display three valence-band (VB) spectra of the Ge(100) 2×1 surface taken along the [010] direction where the experimental band structure has been recently determined unambiguously due to the fact that equivalent $k_{\parallel}$ points are probed along the common $\Gamma J'$ direction of the surface Brillouin zone for the two differently oriented domains of the 2×1 reconstruction.[4] The three emission angles θ_e selected are chosen to emphasize the $S1^0$ surface state with the dominant P_z character identified with the filled dangling-bond band D_{up} of the up atoms of the surface dimers ($\theta_e=11°$), the $S1^0$ surface state together with the energy-dispersive structure A, due to a direct bulk transition[13] ($\theta_e=20°$), and the bulk contribution A together with the $S3^0$ surface state ($\theta_e=39°$) associated with the back-bond state $B2$ mainly localized at the first and second layers below the dimers.[4]

In Fig. 2 we show normal-emission Ge $3d$ core-level spectra taken with $h\nu=75$ eV in a very surface-sensitive

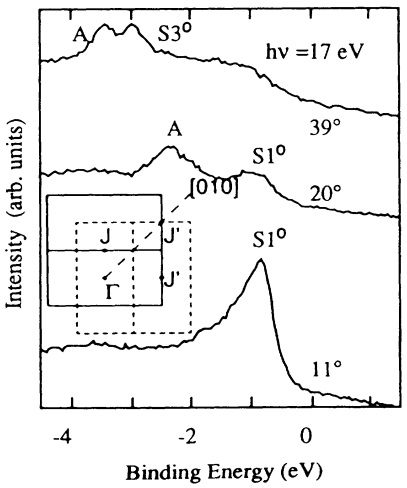

FIG. 1. Valence-band AR photoemission spectra obtained from Ge (100) 2×1 for three emission angles θ_e along the [010] direction. Surface Brillouin zones for the two perpendicular 2×1 domains are shown as an inset. Structures $S1^0$ and $S3^0$ are due to surface states and structure A is due to a direct bulk transition.

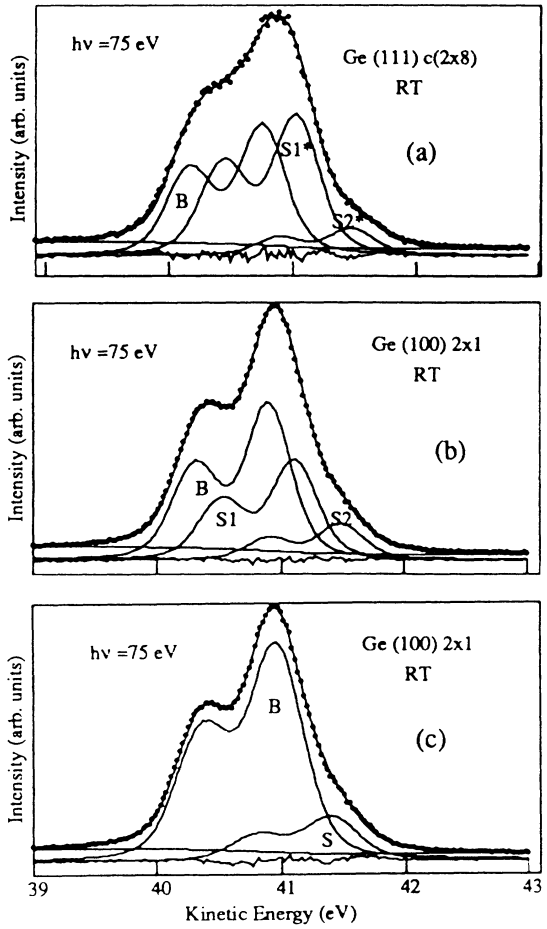

FIG. 2. Angle-resolved photoemission spectra (dots) of the Ge $3d$ core levels taken with a photon energy of 75 eV from (a) the Ge(111) $c(2\times8)$ surface and (b) and (c) the Ge (100) 2×1 surface with identical experimental conditions at normal emission. The solid curves are fit to the data. Both bulk (b) and surface ($S1^*$, $S2^*$, S, $S1$, and $S2$) contributions, as well as the background and the residuals (the difference between the data points and the fitted line), are displayed. For the Ge(100) 2×1 spectra two deconvolutions were carried out; (b) with three spin-orbit doublets of the same width as in (a) for the Ge(111) $c(2\times8)$ surface; (c) with two broadened spin-orbit doublets. Relevant information on these fits is given in Table I.

mode since the kinetic energy of the photoelectrons corresponds to the minimum of the escape length (5 Å) for a Ge(111) $c(2\times8)$ and a Ge(100) 2×1 surface measured in exactly the same experimental conditions. We use the Ge(111) $c(2\times8)$ surface as a reference, since the decomposition of the corresponding Ge $3d$ core-level spectra is now well established,[7,8] to extract true values of the relevant parameters that can be transferred for analysis of the Ge $3d$ core-level spectra of the (100) 2×1 surface.

Core-level spectroscopy is a very powerful method provided it is used in a very rigorous way, since many parameters are involved in the deconvolutions.[14] We decompose the spectra into same-shaped components corresponding to $3d_{3/2}$ and $3d_{5/2}$ spin-orbit doublets. Each line is represented by a Lorentzian whose full width at half maximum (FWHM) correspond to the lifetime of the hole state convolved with a Gaussian whose width is the square root of the quadratic sum of the total instrumental resolution and the further broadening due to other processes, such as inhomogeneous band bending and phonon excitation. The background (BG) of secondary electrons is represented here by an S-shaped function, as proposed by Shirley[15] (while we use a quadratic function at lower photon energies, closer to threshold), whose parameters are adjusted during the least-squares optimization. The closely spaced lines in the Ge $3d$ doublets are assumed to have the same width, so that each doublet is identified by the relative energy and intensity (the branching ratio). The fitting program minimizes the sum of the squares of the residuals. The overall quality of the fit is given by the χ^2 value, which should be as small as possible, and by inspection of the spectrum of the residuals which, for an ideal fit, consists only of the uncorrelated statistical fluctuations of the individual data points. To allow ready comparison, all our confronted spectra were acquired with about the same statistics and then normalized to the same number of counts (one hundred) before deconvolution.

For the RT Ge(111) $c(2\times8)$ surfaces, very good fits could be obtained with two surface components $S1^*$ and $S2^*$, in addition to the bulk one, with a Lorentzian FWHM $L=0.15$ eV and a Gaussian FWHM $G=0.35$ eV, spin-orbit (s.o.) splitting of 0.585 eV and a branching ratio (BR) of 0.66 (i.e., equal to the statistical value of 2/3). The surface components $S1^*$ and $S2^*$ are shifted, by 0.27 and 0.72 eV respectively, toward higher kinetic energy (KE) [or lower binding energy (BE)] as compared to the bulk component. Their relative weights of 46%

TABLE I: Input parameters and results in the Ge $3d$ core-level deconvolutions. BG, background; I, Shirley type; P, second-order polynomial; NSC, number of surface components in the fit; BR, branching ratio; G, Gaussian FWHM in eV; shifts, binding-energy shifts related to the bulk line; weight, relative weight denotes the ratio of the area of the component to the total area; fixed input parameters, lorentzian FWHM, $L=0.15$ eV; spin-orbit splitting of the $3d\,\frac{3}{2}$ and $3d\,\frac{5}{2}$ core levels, s.o.$=0.585$ eV.

		Input parameters				Results		
		BG	NSC	BR	G (eV)	Shifts (eV)	Weight (%)	χ^2
	(111) $c(2\times8)$					S_1^* 0.27	46	
Fig. 2	RT	I	2	0.66	0.35			0.92
						S_2^* 0.73	8	
$h\nu=75$ eV						S_1 0.22	34	
	(100) 2×1		2	0.60	0.35			0.23
$\theta_e=0°$		I				S_2 0.59	12	
	RT		1	0.60	0.42	S 0.43	17	0.41
Fig. 3						S_1 0.22	34	
	(100) 2×1		2	0.60	0.35			0.57
$h\nu=75$ eV		I				S_2 0.57	17	
$\theta_e=60°$	RT		1	0.60	0.42	S 0.44	23	0.57
	(100) $c(4\times2)$					S_1 0.24	21	
Fig. 4	LNT	P	2	0.65	0.33			0.24
$h\nu=52$ eV						S_2 0.56	13	
$\theta_e=0°$	(100) 2×1					S_1 0.24	30	
	RT	P	2	0.65	0.33			0.36
						S_2 0.59	13	
	(100) 2×1					S_1 0.25	28	
Fig. 5		I	2	0.64	0.31			0.52
	RT					S_2 0.60	11	
	(100) 2×1					S_1 0.25	30	
$h\nu=75$ eV		I	2	0.62	0.40			0.62
	540 °C					S_2 0.63	11	
	(100) 1×1					S_1 0.26	33	
$\theta_e=0°$		I	2	0.62	0.45			0.39
	870 °C					S_2 0.64	12	

and 8%, like the energy shifts, are in excellent agreement with previous works.[5,7,8,16–18]. We note that the Gaussian width $G=35$ eV is larger by 0.08 eV than the overall instrumental resolution in this experiment. This extra broadening must be partly due to inhomogeneities, since core-hole-phonon coupling in homopolar semiconductors is rather low both in the bulk[19] and at the surface.[7,16]

We use the same values of L, G, and s.o. as input parameters in the deconvolution of the Ge $3d$ spectra of the Ge(100) 2×1 surface. With a single surface component, as has been considered up to now,[5,6,9,10] this gave very poor fits. To obtain good fits comparable to those obtained on the Ge(111) $c(2\times8)$ surface we had to introduce a second surface component. The two surface components $S1$ and $S2$ are shifted, respectively, by 0.22 and 0.59 eV toward higher KE; they are situated on the same side of the bulk line as the Ge(111) $c(2\times8)$ surface. We emphasize the fact that many spectra at different photon energies and emission angles, for different (100) samples, gave very reproducibly (±0.02 eV) the same positions. At $h\nu=75$ eV the relative weights of $S1$ and $S2$ were about 34% and 12%, respectively. The branching ratio is 0.60, somewhat different from that obtained for the (111) $c(2\times8)$ surfaces, reflecting the influence of the surface crystallographic and electronic states.

Indeed, very good fits could also be obtained with a single surface component S shifted by 0.43 eV towards higher KE, as in previous decompositions, but at the expense of relaxing the constraint on the Gaussian width. With $G=0.42$ eV and a branching ratio of 0.6, we obtained similar χ^2 values as before. However, having analyzed many spectra, we note a slight but systematic preference for the χ^2 values with two surface components (and constrained Gaussian width G) as compared to one (unconstrained G). More significantly, close examination of the residuals always reveals a higher degree of correlation (which is worse) with one surface component than with two. In support of this, we show in Fig. 3 the best comparative deconvolutions of another Ge(100) 2×1 surface (prepared separately). The data were collected with $h\nu=75$ eV and at a polar angle of emission of 60° to emphasize the surface contribution further. The relevant parameters and quantities resulting from the different fits of the core levels in Figs. 2 and 3 are given in Table I. In the following we raise evidence that the introduction of the surface components gives a more consistent decomposition.

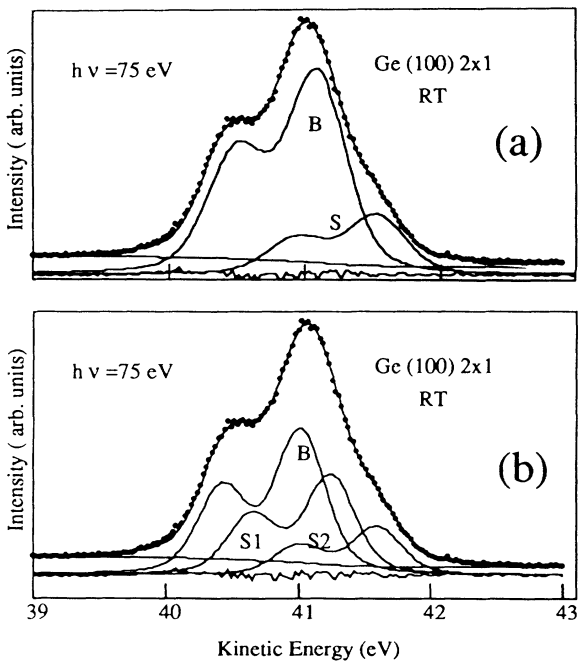

FIG. 3. Comparison (as in Fig. 2) of the deconvolution of the Ge $3d$ core-level spectra of a Ge(100) 2×1 surface with (a) one and (b) two surface components ($h\nu=75$ eV; polar angle of emission is 60°). Relevant information on these fits is given in Table I.

IV. INTERPRETATION OF THE GE $3d$ DECONVOLUTION

The first argument in favor of a decomposition with two surface components, instead of a single one, is that with asymmetric dimers a charge transfer takes place from the down atom to the up atom.[11] Thus, two surface components of equal weight are expected and are actually found on Si(100) 2×1 surfaces.[12] Hence, we assign the $S2$ component at lower binding energy to the up atoms, as proposed in an earlier study,[5] and consequently assume that the down-atom partner is part of the $S1$ component. In this context we meet a situation similar to that of the Ge(111) $c(2\times8)$ surface. There, the $S2^*$ (low-BE) component corresponds to the so-called restatoms [four per unit cell] since, according to the now well-accepted simple adatom reconstruction model in this surface (four adatoms per unit cell),[20–22] a charge transfer takes place from the adatoms to the restatoms.[7,8] The shift produced by the adatoms is contained in the contribution $S1^*$ which also includes the remaining 12 first-layer atoms.

A second argument is that the Gaussian width has to be noticeably broadened (by 0.08 eV) if one single surface component is retained. This argument cannot be justified in either the phonon contribution or the inhomogeneities: the quality of the 2×1 LEED patterns testifies to very well-ordered surfaces and the STM topographs showed a rather low density of defects on the Ge(100) 2×1 surfaces as compared to the Ge(111) $c(2\times8)$ ones.[1]

A third argument stems from the comparison of the relative weights of the different surface components. On the one hand, the single surface component S ($\sim17\%$) at normal emission is supposed to reflect the dimers i.e., a full layer of atoms. On the other hand, the $S1^*$ and $S2^*$ components on the Ge(111) surfaces correspond, respectively, to $\sim46\%$ and $\sim8\%$ (in excellent agreement with the values of Aarts, Hoeven, and Larsen[8] collected at normal emission also). These two components represent, respectively, a monolayer of atoms [four adatoms plus the 12 atoms below them per $c(2\times8)$ cell] and a quarter of a monolayer (four restatoms). Obviously S is too small by about a factor of 2 (as a result of the considerable broadening of the bulk line B) to correspond to its assign-

ment. On the contrary, it is satisfactory to see that with two surface components, taking into account the atomic densities on the (111) and (100) surfaces, the weight of $S2$ on Ge(100) 2×1 is about twice that of $S2^*$ on Ge(111) $c(2\times8)$, in fair agreement with its assignment to the up atoms in the dimers (half a monolayer).

It is also worth commenting on the positions of $S1$ and $S2$. Intuitively, considering the charge transfer involved, one would expect to have the contribution of the down atoms on the other side of the bulk component, as in the case of Si(100) 2×1.[12] However, we note that with the same argument the contribution of the adatoms on the Ge(111) $c(2\times8)$ surface would also be expected at a higher BE, at variance with what is obtained. It is thus likely that for germanium, an important extra-atomic Madelung contribution to the surface core-level shifts reverses the situation.

V. STUDY OF THE REVERSIBLE PHASE TRANSITIONS ON GE (100)

Having established that two surface components are necessary to decompose and interpret consistently the Ge $3d$ core-level spectra of the RT Ge(100) 2×1 surface, we can now turn to the study of the reversible phase transitions that occur on this surface. We first envisage the $c(4\times2)\leftrightarrow2\times1$ transition observed at low temperatures; Fig. 4 shows the atomic placements and the various shifts in these two phases as compared to a 1×1 bulk-terminated arrangement.

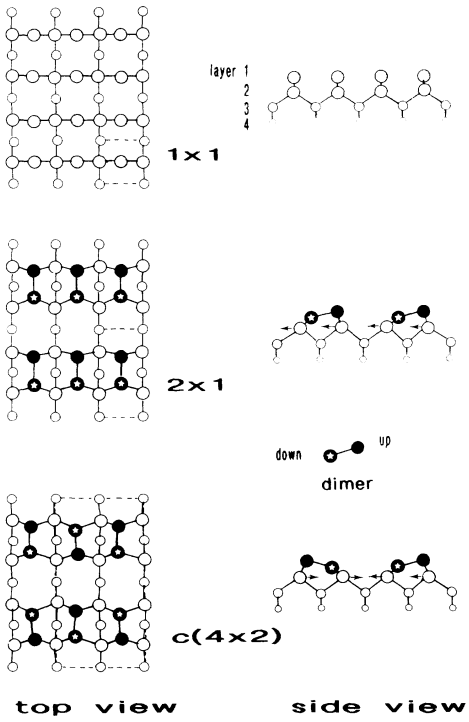

FIG. 4. Atomic placements of the Ge(100) surface: (a) 1×1 bulk-terminated; (b) 2×1; (c) $c(4\times2)$. Arrows indicate the shifts.

A. $c(4\times2)\leftrightarrow2\times1$ phase transition

Considering a dimer as a localized spin, and the buckling orientation to that of the spin, the analogy with an Ising magnet is obvious, as suggested by Ihm *et al.*[23] The sharp $c(4\times2)$ structure observed at low temperatures in LEED corresponds to the antiferromagnetic situation; it is the ground-state configuration.[24]

The stabilization of this lower-energy structure with respect to the 2×1 structure arises from relaxation of the atoms in the layer below the dimers. Looking at Fig. 4, one sees that these atoms move toward the up atom and away from the down atom in the dimers along the $[1\bar{1}0]$ direction to keep the bond length close to the bulk value.

The $c(4\times2)\leftrightarrow2\times1$ phase transition was attributed by Kevan[2] to a demagnetization process: the dimers in a particular row would remain aligned in a one-dimensional antiferromagnetic fashion (besides, this alternation causes the STM images of the rows to appear to

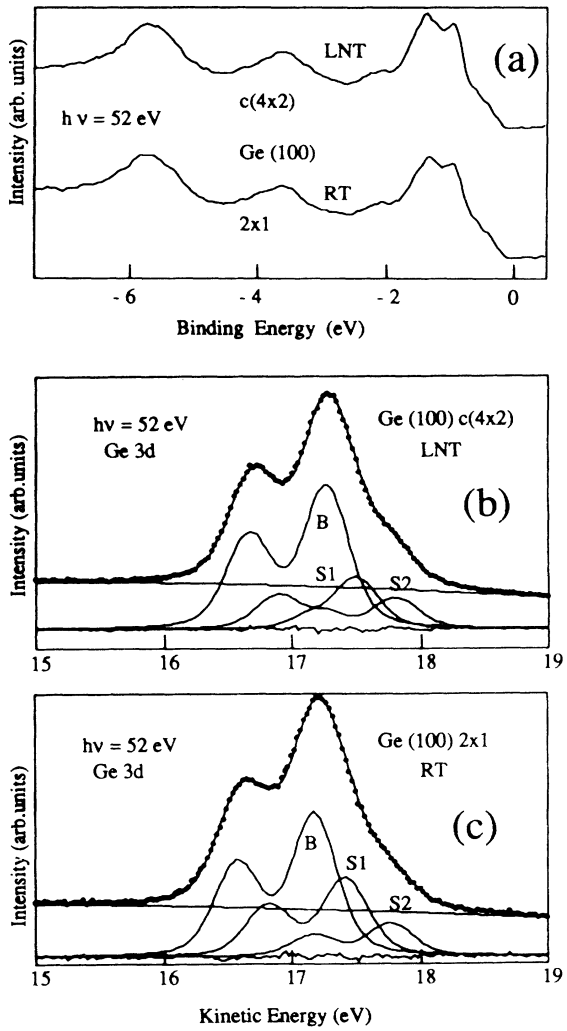

FIG. 5. Photoemission spectra at normal incidence of the $c(4\times2)$ reconstruction at LNT and of the 2×1 reconstruction at RT (a) valence-band spectra taken at $h\nu=52$ eV; (b) Ge $3d$ core-level spectra and their deconvolutions ($h\nu=52$ eV).

wiggle[25]), but the orientation of these dimer rows with respect to one another would become random. An ordered 2×1 structure corresponds comparatively to the ferromagnetic case, while disordering leads to a paramagnetic phase, even though half-order spots may persist due to the huge dimerization energy (~1 eV). We note in passing that the topographic observations just mentioned somehow question the theoretical surface band calculations[4] which rely on an ideal, well-ordered, defect-free, two-dimensionally periodic (ferromagnetic) 2×1 surface. They are also hardly compatible with the measured correlation lengths of 1200 and 1600 Å deduced from the angular width of the $(0,\frac{3}{2})$ and $(\frac{3}{2},0)$ x-ray-diffraction reflections.[3]

In Fig. 5(a) we compare the valence-band spectra of the $c(4\times2)$ reconstruction at LNT and of the 2×1 reconstruction at RT for the same surface; we note only a slight sharpening of the different features at low temperature; in Figs. 5(b) and 5(c) we show the corresponding core-level spectra recorded at normal emission with a photon energy of 52 eV and their deconvolutions. At first no noticeable change is evident. Yet a comparative analysis of several spectra for different surfaces reveals a systematic increase of the weight of the $S1$ component, by 6% on average, when going from the $c(4\times2)$ structure at LNT to the 2×1 structure at RT, all other parameters remaining essentially the same (relevant quantities used in the fit of the spectra of Fig. 5 are given in Table I). We attribute this small increase to the enhanced subsurface strain as pointed out above.

B. $2\times1\leftrightarrow1\times1$ phase transition

In surface x-ray diffraction the high-temperature phase transition is characterized by a sharp drop in the intensities of the half-order peaks at $T_c=682\pm7$ °C, although their FWHM's increase only near the end of the transition, and a strong fall of the specular intensity. This was interpreted in a three-level model assuming the creation of adatoms and vacancies with consequent break up of the dimers.[3]

Photoemission spectroscopy permits direct testing of such a model: in the AR valence-band spectra the strong $S1^0$ and $S3^0$ surface states are clear signatures of the up-atom dangling bonds in the dimers and of their back bonds; in core-level spectra the low-BE component also corresponds to the up atoms. These features are thus directly correlated to the presence of the dimers. If the $2\times1\leftrightarrow1\times1$ phase transition is really due to the destruction of the dimers, there should be a proportional decrease of the intensity of the $S2$-shifted component (since core-level spectroscopy is essentially a local probe) and correlatively a drop in the intensity of both $S1^0$ and $S3^0$ valence-band surface states (here direct proportionality cannot be assumed: since VB photoemission is rather a medium range probe, it is even likely that the fall in intensity would be much faster than a simple linear relation).

We have thus recorded photoemission spectra at two elevated temperatures: at 540 °C, below the phase transition (2×1-LEED pattern), and at 870 °C, above it (1×1 pattern). These values, estimated from our thermocouple readings (due to its location, the thermocouple measured actual temperatures lower than those of the sample surfaces), were cross-checked with the temperature dependence of bulk transition A. In Fig. 6 we show VB spectra of the same surface measured first at a takeoff angle of 11° to follow the temperature behavior of the $S1^0$ surface state and, next at 39° emission angle, to follow that of the $S3^0$ surface state in comparison with that of bulk transition A. In Fig. 7 we display the Ge $3d$ core-level spectra recorded at the same temperatures, and their deconvolutions. Obviously, both types of spectra are markedly broadened as compared to RT spectra. This broadening is caused by stray fields and drifts in the electronics due to the heating: we measured the same broadening of the Fermi edge of the tantalum foil in contact with the sample. The Ge $3d$ core-level spectra were thus decomposed with enlarged Gaussians as indicated in Table I. Nevertheless, the fits are still very good and lead essentially to the same type of decomposition at 540° (2×1 phase) and at 870° (1×1 phase) as at RT. The only change is a small increase of the weight of the $S1$ component (by 7% on average at $h\nu=75$eV) as determined at several photon energies on two different initial surfaces. The most remarkable point is that the weight of the $S2$ component remains the same past the transition temperature. This is a clear indication that the number of dimers has not significantly changed.

The same conclusion may be drawn from the evolution of the valence-band spectra. Clearly, despite the broadening, the surface states $S1^0$ and $S3^0$ persist, although with some attenuation.

The temperature dependence of VB photoemission can be constructed by viewing photoemission as a scattering process.[26,27] This photoelectron scattering event can be described by a static factor containing a Debye-Waller factor $\exp-2M$, where $M=Bq^2/4\pi^2$ and q is the scattering vector.[28]

The peak-to-background ratio H/BG of the $S1^0$ surface state (the peak height is measured from a linear ex-

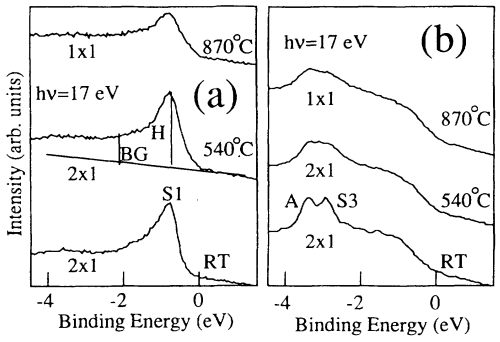

FIG. 6. Temperature-dependent valence-band photoemission spectra ($h\nu=17$ eV) at two polar angles of emission: (a) 11° to follow the height of the $S1^0$ surface state, as compared to the background BG; (b) 39° to follow the $S3^0$ surface state with respect to the bulk transition A at RT, at 540 °C (2×1 phase), and at 870 °C past the phase transition temperature (1×1 phase).

trapolation of the BG above the Fermi level; the BG is taken at 2 eV below the peak, as shown in Fig. 6), as well as the intensity ratio of the $S3^0$ surface state to the bulk transition A (for this, both peaks are modeled as Voigt functions lying over a quadratic background), are plotted in logarithmic scale in Fig. 8. From the linear variations, with $q = 1.11$ Å^{-1}, we obtain a rms displacement $\langle u^2 \rangle^{1/2}$ at 300 K of 0.20 Å from the $S1^0$ intensity variations and 0.18 Å from the $S3^0$ intensity variations, assuming for the A peak a B factor equal to that of bulk germanium: $B = 0.57$ Å^2.[29] Taking into account our estimated error bars and limited data set, these results are in fair agreement with the determination of Johnson *et al.*[3] by x-ray diffraction: 0.15 ± 0.05 Å, that is, about twice the bulk Ge value. This proves again that the number of dimers is not significantly altered at the $2\times1 \leftrightarrow 1\times1$ phase transition.

We also stress that in a previous study by *in situ* ellipsometry (which is a very surface-sensitive local probe) of the high-temperature phase transitions of the clean Ge(111) surface,[30] we have compared, in the same experimental situation, the temperature behaviors of the ellipsometric angles for Ge(111) and Ge(100) samples (see Fig. 6 in paper 30). While two transitions around 700 and 800 °C were clearly evidenced for Ge(111), a constant value was obtained for Ge(100) in the temperature region explored: 600–850 °C. The constancy of the signal testified to the conservation of the number of dimers in a temperature domain where the $2\times1 \leftrightarrow 1\times1$ phase transition takes place.

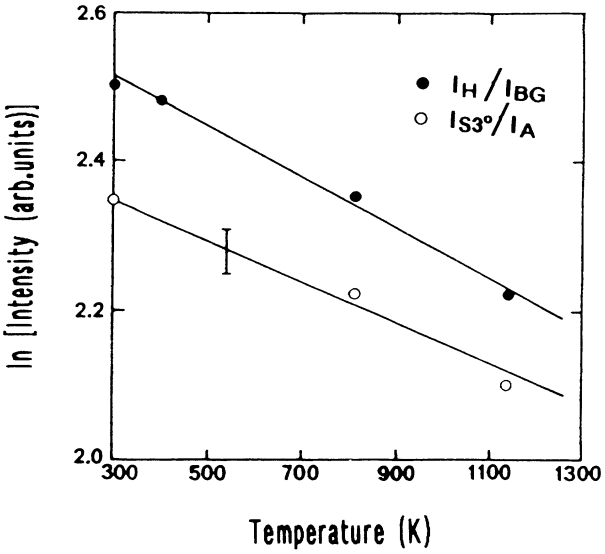

FIG. 8. The peak (H) to background (BG) ratio of the $S1^0$ surface state and the ratio of the intensities of the $S3^0$ and A features are plotted vs temperature in the ln scale.

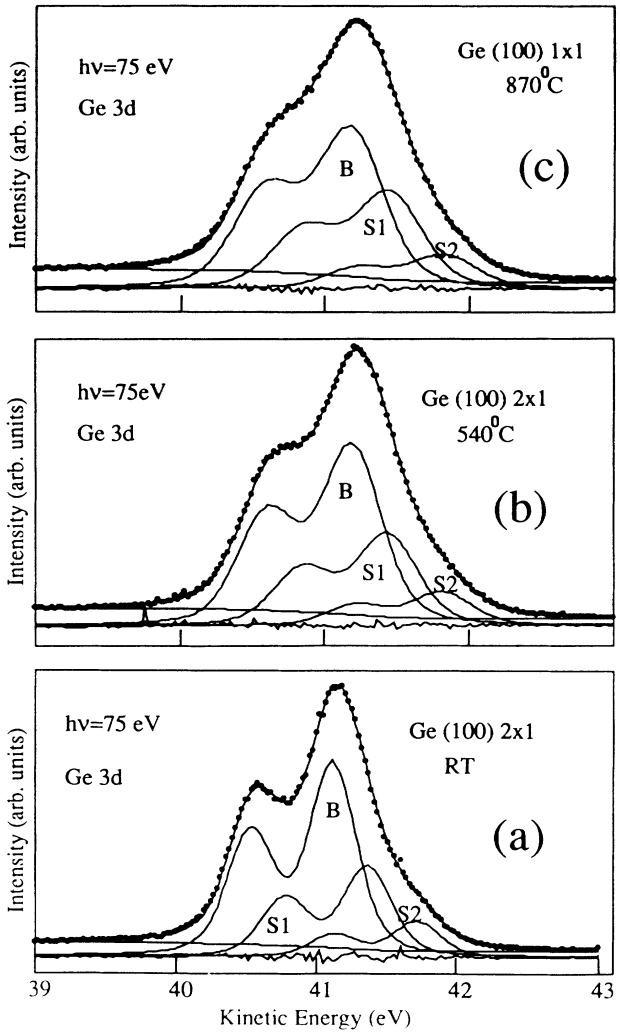

FIG. 7. Ge 3d core-level spectra and their deconvolutions at (a) RT, (b) 540 °C, and (c) 870 °C.

Indeed, this conservation challenges the model with breakup of surface dimers proposed by Johnson *et al.*[3] Since we noticed an increase of the weight of the $S1$ component in the Ge core levels, we think that, in fact, the $2\times1 \leftrightarrow 1\times1$ phase transition is accompanied by more subsurface strain. This may originate in a paramagnetic type of disordering of the dimers as was predicted in the theoretical study of Ihm *et al.*[23]

VI. CONCLUSION

In summary, we have proved that a consistent deconvolution of the Ge 3d core-level spectra of the clean Ge(100)2×1 reconstructed surface at RT requires two surface components: $S1$ at -0.23 eV binding energy relative to the bulk line B, and $S2$ at -0.60 eV. This last component is attributed to the up-atoms in the asymmetric dimers.

No drastic changes in both valence band and core-level photoemission take place upon passing the phase transitions from the $c(4\times2)$ reconstruction at low temperatures to the 2×1 one at RT or to the 1×1 structure at high temperatures. In this last case the number of dimers is essentially conserved. Each transition is accompanied by an increase in the subsurface strain upon going from the ground-state antiferromagnetic-type $c(4\times2)$ configuration of the dimers at LNT, through the 2×1 structure at RT and to the high-temperature disordered

(paramagneticlike) arrangement of the dimers at high temperature.

ACKNOWLEDGMENTS

We greatly acknowledge the assistance of Dr. M. Haruki in the photoemission experiments at MAX-Lab and in the core-level deconvolutions as well as the participation of Professor A. Kahn and Dr. J. E. Bonnet in the measurements in LURE. We thank Professor J. Derrien, Dr. J. Chevrier, and Dr. N. Motta for fruitful discussions. The skilled technical help of Lars Ilver was very much appreciated. We have enjoyed the efficient working atmosphere at MAX-Lab, help from the staff, and several discussions with many researchers. We fully acknowledge the support of the Swedish Natural Science Research Council for this work. The CRMC2 is "Unité Propre du Centre National de la Recherche Scientifique No. 7251."

---

*Also at Unité de Formation et de Recherche sciences de la Matière, Université de Provence, Marseille, France.

[1]J. A. Kubby, J. E. Griffith, R. S. Becker, and J. S. Vickers, Phys. Rev. B **36**, 6079 (1987).

[2]S. D. Kevan, Phys. Rev. B **32**, 2344 (1985).

[3]A. D. Johnson, C. Norris, J. W. M. Frenken, S. Derbyshire, J. E. MacDonald, R. G. Van Silfhout, and J. F. Van der Veen, Phys. Rev. B **44**, 1134 (1991).

[4]E. Landemark, R. I. G. Uhrberg, P. Krüger, and J. Pollmann, Surf. Sci. Lett. **236**, L359 (1990).

[5]R. D. Schnell, F. J. Himpsel, A. Bogen, D. Rieger, and W. Steinmann, Phys. Rev. B **32**, 8052 (1985).

[6]T. Miller, A. P. Shapiro, and T. C. Chiang, Phys. Rev. B **31**, 7915 (1985).

[7]K. Hricovini, G. Le Lay, M. Abraham, and J. E. Bonnet, Phys. Rev. B **41**, 1258 (1990).

[8]J. Aarts, A. J. Hoeven, and P. K. Larsen, Phys. Rev. B **38**, 3925 (1988).

[9]T. Miller, E. Rosenwinkel, and T. C. Chiang, Solid State Commun. **47**, 935 (1983).

[10]K. Hricovini, G. Le Lay, A. Kahn, A. Taleb-Ibrahimi, and J. E. Bonnet, in *The Structure of Surfaces III,* edited by S. Y. Tong, N. A. Van Hove, K. Takayanagi, and X. D. Xie, Springer Series in Surface Sciences Vol. 24 (Springer-Verlag, Berlin, 1991), p. 589.

[11]D. J. Chadi, Phys. Rev. Lett. **43**, 43 (1979).

[12]G. K. Werheim, D. M. Riffe, J. E. Rowe and P. H. Citrin, Bull. Am. Phys. Soc. **36**, 808 (1991).

[13]T. C. Hsieh, T. Miller, and T. C. Chiang, Phys. Rev. B **30**, 7005 (1984).

[14]J. J. Joyce, M. Del Giudice, and J. H. Weaver, J. Electron Spectrosc. Relat. Phenom. **49**, 31 (1989).

[15]D. A. Shirley, Phys. Rev. B **5**, 4709 (1972).

[16]S. B. Dicenzo, P. A. Bennet, D. Tribula, P. Thiry, G. K. Wertheim, and J. E. Rowe, Phys. Rev. B **31**, 2330 (1985).

[17]T. Miller, T. C. Hsieh, and T. C. Chiang, Phys. Rev. B **33**, 6938 (1986).

[18]A. L. Wachs, T. Miller, A. P. Shapiro, and T. C. Chiang, Phys. Rev. B **35**, 5514 (1987).

[19]R. D. Carson and S. E. Schatterly, Phys. Rev. B **39**, 1659 (1989).

[20]R. Feidenhans'l, J. S. Pedersen, J. Bohr, and M. Nielson, Phys. Rev. B **38**, 9715 (1988).

[21]P. M. Marée, N. Nakagawa, and J. F. Van der Veen, Phys. Rev. B **38**, 1585 (1988).

[22]R. S. Becker, B. S. Swartzentruber, J. S. Vickers, and T. Klisner, Phys. Rev. B **39**, 1633 (1989).

[23]J. Ihm, D. H. Lee, J. D. Joannopoulos, and J. J. Xiong, Phys. Rev. Lett. **58**, 1872 (1983).

[24]M. Needels, M. C. Payne and J. D. Joannopoulos, Phys. Rev. Lett. **58**, 1765 (1987).

[25]J. E. Griffith and G. P. Kochanski, Solid State Mater. Sci. **16**, 255 (1990).

[26]N. J. Shevchik, Phys. Rev. B **16**, 3428 (1977).

[27]B. P. Tonner, H. Li, M. J. Robrecht, and Y. C. Chou, Phys. Rev. B **34**, 4386 (1986).

[28]B. E. Warren, *X-ray Diffraction* (Addison-Wesley, London, 1969).

[29]B. W. Batterman and M. Chipman, Phys. Rev. **127**, 690 (1962).

[30]M. Abraham, G. Le Lay, and J. Hila, Phys. Rev. B **41**, 9828 (1990).